ELSEVIER

International Journal of Solids and Structures 41 (2004) 3999–4024

INTERNATIONAL JOURNAL OF SOLIDS and STRUCTURES

www.elsevier.com/locate/ijsolstr

A local method for solutions in two-dimensional potential theory and linear elasticity

Salil S. Kulkarni [a,*,1], Subrata Mukherjee [a,*], Mircea D. Grigoriu [b]

[a] *Department of Theoretical and Applied Mechanics, Cornell University, Ithaca, NY 14853, USA*
[b] *Department of Environmental and Civil Engineering, Cornell University, Ithaca, NY 14853, USA*

Received 14 March 2003; received in revised form 10 February 2004
Available online 27 March 2004

Abstract

A numerical method called the Boundary Walk Method (BWM) is used to solve problems in two-dimensional potential theory and linear elasticity in multiply connected domains. The BWM is a local method in the sense that it directly gives the solution at the point of interest. It is based on a global integral representation of the unknown function in the form of a potential, followed by evaluating the integrals in the resulting series solution using Monte Carlo simulation. Appropriate integral formulations which can be used with the BWM to solve problems in potential theory and linear elasticity in multiply-connected domains are presented. Numerical results for some sample problems based on these formulations are also presented.
© 2004 Elsevier Ltd. All rights reserved.

Keywords: Local method; Potential theory; Linear elasticity; Multiply-connected domain; Monte Carlo integration

1. Introduction

Local numerical methods solve a given boundary value problems at the point of interest directly and generally do not need any discretization of the domain/surface, in contrast with global methods like the Finite Element and the Boundary Element Methods. Local methods are inherently parallel and hence much less programming effort is required to parallelize a code when compared with either the FEM or the BEM. A main disadvantage of local methods is their rather limited applicability (at present) when compared to the FEM or the BEM. Increasing the versatility of local methods is a matter of continuing research. It is not clear at this stage if local methods will someday become competitive with established methods such as the BEM and FEM. Efforts in this direction, however, are considered to be worthwhile by the present authors.

The local method described in this paper is called a Boundary Walk Method (BWM) since it simulates a random walk on the boundary of the domain. It is based on a global integral representation of the solution

* Corresponding authors. Tel.: +1-847-467-3154; fax: +1-847-491-5227.
E-mail addresses: sm85@cornell.edu (S. Mukherjee), salil@northwestern.edu (S.S. Kulkarni).
[1] Present address: Department of Mechanical Engineering, Northwestern University, 2145 Sheridan Road, Evanston, IL 60208, USA.

0020-7683/$ - see front matter © 2004 Elsevier Ltd. All rights reserved.
doi:10.1016/j.ijsolstr.2004.02.023

in a form of a potential. The solution of the integral equation of the corresponding density is sought in the form of a power series. The individual terms in the series are then evaluated using Monte Carlo integration. This avoids any meshing and leads to an accurate implementation of the problem geometry and boundary conditions. It also avoids the 'curse of dimensionality' associated with classical quadrature schemes (see Evans and Swartz, 2000). The BWM with appropriate integral formulations was earlier applied to solve problems in two-dimensional potential theory and elasticity in convex domains and the details can be found in Kulkarni et al. (2003). A description of the BWM in three-dimensions for potential theory and linear elasticity can be found in Sabelfeld (1991), Sabelfeld and Simonov (1994) but the texts deal mainly with problems in simply-connected domains for linear elasticity. They do discuss the application of the BWM to solve problems in multiply-connected domains in potential theory but the integral formulations are different than those used here. Shia and Hui (2000) have described a similar method for solving traction prescribed problems in linear elasticity based on the direct integral formulation of Rizzo (1967), while indirect formulations are used for both displacement and traction prescribed problems in the current work.

The main contribution of the current paper is the presentation of integral formulations for problems in multiply-connected domains in both potential theory and linear elasticity which are appropriate for use with the BWM. These formulations are then used in conjunction with the BWM to solve some sample problems.

The remainder of the paper is organized as follows. Section 2 presents the theoretical background of the BWM. Section 3 describes the solutions of Dirichlet and Neumann problems in potential theory using the BWM. Section 4 describes the solutions of the displacement and traction prescribed problems in linear elasticity using the BWM. Section 5 presents numerical results obtained by applying the BWM to solve some test problems. This is followed by concluding remarks in Section 6. Finally, a proof of an observation made during the numerical implementation of the BWM appears in Appendix A.

2. Theoretical background

This section describes the theoretical details of the Boundary Walk Method. It is divided into three parts. The first part describes the class of problems which can be solved using the BWM and the basic procedure followed in obtaining the required solution. The second part defines the estimators used to evaluate the multi-dimensional integrals occurring in the solution. The third part describes the densities used in generating the random variables which are employed in constructing the estimators.

2.1. Solution of an integral equation

The Boundary Walk Method is mainly concerned with evaluating integrals of the type

$$I(\mathbf{x}_0) = \int_\Gamma R(\mathbf{x}_0, \mathbf{y})\mu(\mathbf{y})\mathrm{d}S(\mathbf{y}), \quad \mathbf{x}_0 \in D, \tag{1}$$

where the density $\mu(\mathbf{y})$ satisfies the integral equation

$$\mu(\mathbf{y}) = \lambda \int_\Gamma K(\mathbf{y}, \mathbf{y}')\mu(\mathbf{y}')\mathrm{d}S(\mathbf{y}') + f(\mathbf{y}), \quad \mathbf{y} \in \Gamma \equiv \partial D. \tag{2}$$

Here D is the domain of interest, Γ is the boundary of the domain and $\lambda \in \mathbb{R}$ is a parameter. The functions $R(\mathbf{x}, \mathbf{y})$, $K(\mathbf{x}, \mathbf{y})$, $\mu(\mathbf{y})$, $f(\mathbf{y})$ and $I(\mathbf{x})$ are assumed to be real valued. For the case of simplicity it will be assumed that all the functions are continuous.

Eq. (2) is solved by assuming that $\mu(\mathbf{y})$ can be represented in a uniformly convergent series of the form (e.g. see Sobolev, 1964)

$$\mu(\mathbf{y}) = \mu_0(\mathbf{y}) + \lambda\mu_1(\mathbf{y}) + \lambda^2\mu_2(\mathbf{y}) + \cdots. \tag{3}$$

Substituting Eq. (3) into Eq. (2) and equating equal powers of λ, one obtains

$$\begin{aligned}
&\mu_0(\mathbf{y}) = f(\mathbf{y}),\\
&\mu_1(\mathbf{y}) = \int_\Gamma K(\mathbf{y},\mathbf{y}_1) f(\mathbf{y}_1)\mathrm{d}S(\mathbf{y}_1),\\
&\mu_2(\mathbf{y}) = \int_\Gamma \int_\Gamma K(\mathbf{y},\mathbf{y}_1)K(\mathbf{y}_1,\mathbf{y}_2) f(\mathbf{y}_2)\mathrm{d}S(\mathbf{y}_2)\mathrm{d}S(\mathbf{y}_1),\\
&\vdots\\
&\mu_k(\mathbf{y}) = \underbrace{\int_\Gamma \cdots \int_\Gamma}_{k \text{ times}} K(\mathbf{y},\mathbf{y}_1)\cdots K(\mathbf{y}_{k-1},\mathbf{y}_k) f(\mathbf{y}_k)\mathrm{d}S(\mathbf{y}_k)\cdots \mathrm{d}S(\mathbf{y}_1).
\end{aligned} \tag{4}$$

(Note the iterative nature of the integrals appearing in Eq. (4).) The solution to Eq. (1) is obtained by multiplying Eq. (3) by $R(\mathbf{x}_0,\mathbf{y})$ and then integrating the result over the boundary. Hence the solution to Eq. (1) can be written as

$$I(\mathbf{x}_0) = \sum_{n=0}^{\infty} \lambda^n I_n(\mathbf{x}_0), \tag{5}$$

where

$$I_k(\mathbf{x}_0) = \underbrace{\int_\Gamma \cdots \int_\Gamma}_{k+1 \text{ times}} R(\mathbf{x}_0,\mathbf{y}_0)K(\mathbf{y}_0,\mathbf{y}_1)K(\mathbf{y}_1,\mathbf{y}_2)\cdots K(\mathbf{y}_{k-1},\mathbf{y}_k) f(\mathbf{y}_k)\mathrm{d}S(\mathbf{y}_k)\cdots \mathrm{d}S(\mathbf{y}_1)\mathrm{d}S(\mathbf{y}_0), \quad k = 0,1,\ldots$$

2.2. Monte Carlo integration

Monte Carlo integration is used to evaluate the individual terms in Eq. (5). The Monte Carlo method used in the present paper (see Rubinstein, 1981) efficiently exploits the iterative nature of the individual terms and is briefly described below.

Let $\mathbf{Y} = \{\mathbf{Y}_0, \mathbf{Y}_1, \ldots, \mathbf{Y}_n, \ldots\}$ be a Γ-valued Markov chain. One particular realization of the chain is illustrated in Fig. 1. The initial state $\mathbf{Y}_0$ has a density $p_0(\mathbf{Y}_0)$. The following states of $\mathbf{Y}$ are defined by the transition density $p(\cdot|\mathbf{y}_{i-1})$, i.e., the density of the conditional random variable $\mathbf{Y}_i\,|\,(\mathbf{Y}_{i-1} = \mathbf{y}_{i-1})$. Hence $p_0(\mathbf{y}_0)\mathrm{d}S(\mathbf{y}_0)$ can be interpreted as the probability of going from the given point $\mathbf{x}_0$, to a neighborhood

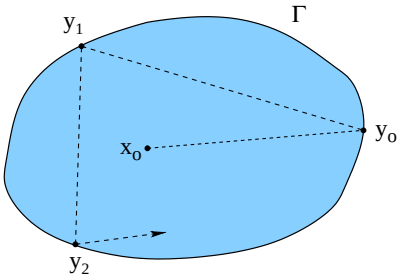

Fig. 1. Boundary walk method.

$\mathrm{d}S(\mathbf{y}_0)$ of the point $\mathbf{y}_0$. Similarly $p(\mathbf{y}_i\,|\,\mathbf{y}_{i-1})\mathrm{d}S(\mathbf{y}_i)$ can be interpreted as the probability of going from point $\mathbf{y}_{i-1}$ to a neighborhood $\mathrm{d}S(\mathbf{y}_i)$ of the point $\mathbf{y}_i$ given point $\mathbf{y}_{i-1}$. The choice of $p_0(\mathbf{y}_0)$ and $p(\mathbf{y}_i\,|\,\mathbf{y}_{i-1})$ is subject only to the constraints

$$p_0(\mathbf{y}_0) > 0 \quad \text{if } R(\mathbf{x}_0, \mathbf{y}_0) \neq 0,$$
$$p(\mathbf{y}_i\,|\,\mathbf{y}_{i-1}) > 0 \quad \text{if } K(\mathbf{y}_{i-1}, \mathbf{y}_i) \neq 0.$$

Note that the constraint ensures that the random variable has a finite mean. Then

$$E[\zeta_k] = I_k(\mathbf{x}_0), \tag{6}$$

where the random variable

$$\zeta_k = \frac{R(\mathbf{x}_0, \mathbf{Y}_0)}{p_0(\mathbf{Y}_0)} W_k f(\mathbf{Y}_k) \tag{7}$$

has density $p_0(\mathbf{Y}_0)p(\mathbf{Y}_1\,|\,\mathbf{Y}_0)\cdots p(\mathbf{Y}_k\,|\,\mathbf{Y}_{k-1})$ and

$$W_k = W_{k-1}\frac{K(\mathbf{Y}_{k-1}, \mathbf{Y}_k)}{p(\mathbf{Y}_k\,|\,\mathbf{Y}_{k-1})}, \quad W_0 \equiv 1.$$

The proof of Eq. (6) is given in Appendix A. The random variable defined in Eq. (7) is then used to construct a direct estimator given by

$$\hat{I}^{\mathrm{D}}_{k,N} = \frac{1}{N}\sum_{i=1}^{N} \zeta_k^i. \tag{8}$$

where ζ_k^i is the ith sample used to evaluate the kth term in the series given by Eq. (5).

Similar to Eq. (6), one also has

$$E[\zeta_k^*] = I_k(\mathbf{x}_0), \tag{9}$$

where the random variable

$$\zeta_k^* = R(\mathbf{x}_0, \mathbf{Y}_k) W_k^* \frac{f(\mathbf{Y}_0)}{p_0(\mathbf{Y}_0)} \tag{10}$$

has density $p_0(\mathbf{Y}_0)p(\mathbf{Y}_1\,|\,\mathbf{Y}_0)\cdots p(\mathbf{Y}_k\,|\,\mathbf{Y}_{k-1})$ and

$$W_k^* = \frac{K^*(\mathbf{Y}_{k-1}, \mathbf{Y}_k)}{p(\mathbf{Y}_k\,|\,\mathbf{Y}_{k-1})} W_{k-1}^*, \quad W_0^* \equiv 1.$$

Here $K^*(\mathbf{y}, \mathbf{y}')$ is the adjoint kernel corresponding to kernel in Eq. (2). Note that the proof for Eq. (9) follows from the following relation:

$$\int_\Gamma \phi(\mathbf{y})\left(\int_\Gamma K(\mathbf{y}, \mathbf{y}')\psi(\mathbf{y}')\mathrm{d}S(\mathbf{y}')\right)\mathrm{d}S(\mathbf{y}) = \int_\Gamma \psi(\mathbf{y})\left(\int_\Gamma K^*(\mathbf{y}, \mathbf{y}')\phi(\mathbf{y}')\mathrm{d}S(\mathbf{y}')\right)\mathrm{d}S(\mathbf{y}).$$

where $\phi(\mathbf{y})$ and $\psi(\mathbf{y})$ are two real valued functions defined on Γ. The random variable defined in Eq. (10) is used to construct an adjoint estimator given by

$$\hat{I}^{\mathrm{A}}_{k,N} = \frac{1}{N}\sum_{i=1}^{N} \zeta_k^{*i}, \tag{11}$$

where $\zeta_k^{*^i}$ is the ith sample used to evaluate the kth term in the series, given by Eq. (5).

A few known properties of the the estimators defined above are summarized next. For details refer to one of the many books available on Monte Carlo integration (see for e.g., Evans and Swartz, 2000). Both the estimators will henceforth be represented by

$$\hat{I}_{k,N} = \frac{1}{N}\sum_{i=1}^{N} X_k^i, \tag{12}$$

where X_i's are independent identically distributed (iid) random variables with mean $\mu = I_k(\mathbf{x}_0)$ and variance σ^2.

First note that

$$E[\hat{I}_{k,N}] = I_k(\mathbf{x}_0), \quad \text{for all } N \geqslant 1.$$

Therefore $\hat{I}_{k,N}$ is an *unbiased* estimator. The variance of the estimator decreases linearly with N (assuming $\sigma^2 < \infty$) and is given by

$$\mathrm{Var}[\hat{I}_{k,N}] = \frac{\sigma^2}{N}.$$

The estimator is also a *consistent estimator* because

$$\lim_{N\to\infty} \mathrm{Var}[\hat{I}_{k,N}] = 0.$$

Bounds on the absolute error can be obtained by the central limit theorem according to which the estimator $\hat{I}_{k,N}$ has a normal distribution asymptotically, with mean μ and standard deviation $\sigma/\sqrt{N}$, i.e.

$$\frac{\hat{I}_{k,N} - \mu}{\sigma/\sqrt{N}} \to^D Z$$

as $N \to \infty$, where $Z \sim \mathrm{Normal}(0,1)$. The variance σ^2 is usually estimated using

$$s^2 = \frac{1}{N-1}\sum_{i=1}^{N}\left(X_k^i - \hat{I}_{k,N}\right)^2$$

and one also has

$$\frac{\hat{I}_{k,N} - \mu}{s/\sqrt{N}} \to^D Z.$$

Finally note that the Monte Carlo integration will converge even if the variance is infinite, provided $I_k(\mathbf{x}_0)$ is finite. This is guaranteed from the strong law of large numbers

$$P\left(\lim_{N\to\infty} \hat{I}_{k,N} = I_k(\mathbf{x}_0)\right) = 1,$$

which says that for a large sample size N, $\hat{I}_{k,N}$ will be a good approximation to $I_k(\mathbf{x}_0)$.

Two types of error estimates are used in the current work to get a bound on the error when using the estimator given by Eq. (12). They are:

- *Standard deviation of the sample mean*, $\widehat{s_t}$. $\widehat{s_t}$ is estimated by
$$\widehat{s_t} = s/\sqrt{N}.$$
- *Coefficient of Variation (CV)*. The CV is defined to be the ratio of the standard deviation and the mean and is estimated by
$$\mathrm{CV} \approx \frac{1}{\sqrt{N}}\frac{s}{\hat{I}_{k,N}}.$$

This estimate is useful only when $\mu = I_k(\mathbf{x}_0) \neq 0$. The advantage of this error estimator as compared to the standard deviation is that it is a dimensionless quantity and scale invariant.

2.3. Densities

The initial and transition densities used in the current paper in estimating the integrals are described next.

Let $\mathbf{x}_0$ be any point in the plane. Let L_i, $i = 1, \ldots, N$, be N nonintersecting closed curves in the plane. Consider the curve L_k. Let $\mathbf{p}_j$, $j = 1, \ldots, M$, be M points on L_k where the term $\cos(\phi_{\mathbf{y},\mathbf{x}_0})$ changes sign. Here $\mathbf{y}$ is a point on the curve L_k and $\phi_{\mathbf{y},\mathbf{x}_0}$ denotes the angle between the ray from the point $\mathbf{x}_0$ to the point $\mathbf{y}$ and the outward normal at point $\mathbf{y}$. Then the total angle subtended by the curve L_k is defined by

$$\begin{aligned}\Omega^k_{\mathbf{x}_0} &= \int_{L_k} \frac{|\cos(\phi_{\mathbf{y},\mathbf{x}_0})|}{r}\,\mathrm{d}S(\mathbf{y}),\\ &= \sum_{j=1}^{M} \int_{\mathbf{p}_j}^{\mathbf{p}_{j+1}} \frac{|\cos(\phi_{\mathbf{y},\mathbf{x}_0})|}{r}\,\mathrm{d}S(\mathbf{y}), \quad (\text{here } \mathbf{p}_{M+1} = \mathbf{p}_1),\\ &= \sum_{j=1}^{M} \omega^k_j.\end{aligned}$$

The total angle subtended by the N curves at the point $\mathbf{x}_0$ is defined as the sum of the total angles subtended by the individual curves at the point $\mathbf{x}_0$ and is therefore given by

$$\Omega_{\mathbf{x}_0} = \sum_{i=1}^{N} \Omega^i_{\mathbf{x}_0}.$$

Fig. 2 illustrates the concept of the total angle subtended at a point $\mathbf{x}_0$ in a doubly-connected region. The probability of going from the point $\mathbf{x}_0$ to a neighbourhood, $\mathrm{d}S(\mathbf{y}_0)$, of the point $\mathbf{y}_0$ which is uniformly distributed (angle measure) is then given by

$$p(\mathbf{y}_0\,|\,\mathbf{x}_0)\mathrm{d}S(\mathbf{y}_0) = \frac{\mathrm{d}\omega}{\Omega_{\mathbf{x}_0}} = \frac{|\cos(\phi_{\mathbf{y}_0,\mathbf{x}_0})|}{\Omega_{\mathbf{x}_0} r}\,\mathrm{d}S(\mathbf{y}_0).$$

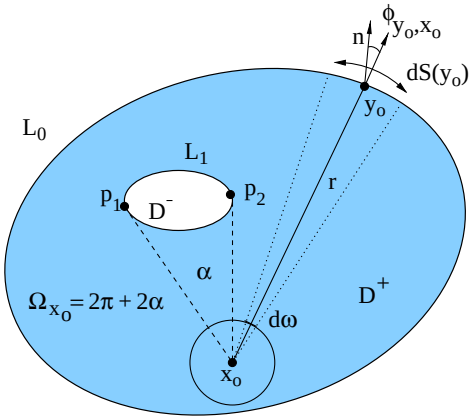

Fig. 2. The total angle subtended at a point.

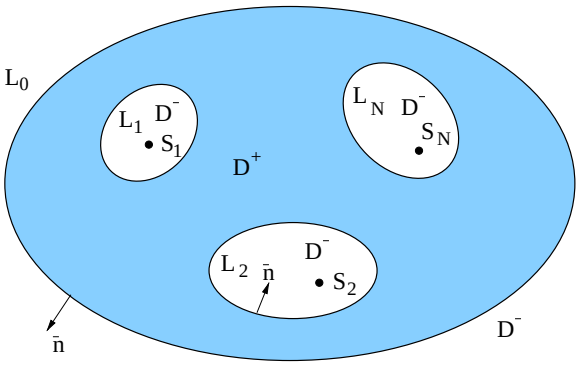

Fig. 3. Multiply-connected domain.

Hence,

$$p(\mathbf{y}_0 \,|\, \mathbf{x}_0) = \frac{|\cos(\phi_{\mathbf{y}_0,\mathbf{x}_0})|}{\Omega_{\mathbf{x}_0} r}.$$

The point $\mathbf{y}_0$ is chosen by first selecting a number which is uniformly distributed in the interval $[0, \Omega_{\mathbf{x}_0}]$ and then shooting a ray from the point $\mathbf{x}_0$ in the appropriate direction. This direction takes into account the total angles subtended by each closed curve L_k and the segments ω_j^k associated with that curve. Both the initial and transition densities needed to calculate the individual terms in the series are obtained from the procedure explained above since no assumption is made regarding the location of point $\mathbf{x}_0$.

Remark. In order to apply the Boundary Walk Method presented in this paper to numerically solve problems arising in potential theory and linear elasticity, one must start with integral formulations which satisfy the following requirements:

1. The integral equations should be of the form as shown in Eqs. (1) and (2) so that they can be solved using the procedure described in Section 2.1.
2. Kernels which appear in the integral equation of the second kind need to be weakly singular so that the densities defined in Section 2.3 can be used to evaluate the integrals. The use of such kernels along with the mentioned densities leads to estimators with finite variance due to the cancellation of the singularities. This requirement of finite variance is essential if one wants to use get bounds on the errors incurred when using Monte Carlo integration.

A consequence of these requirements is that one must start with suitable integral formulations depending on the type of domain and boundary conditions under consideration.

Integral formulations for solutions in the multiply-connected domain D^+ shown in Fig. 3 are presented next. The outer boundary of D^+ is L_0 while the interior boundary curves are $L_1, \ldots, L_N$, and $L = L_0 \cup L_1 \cup \cdots \cup L_N$. The normal is assumed to point into the region denoted by D^-.

3. Solutions of problems in potential theory using the BWM

3.1. Interior Dirichlet problem in a multiply-connected domain

The interior Dirichlet problem involves the determination of a function $u(\mathbf{x})$ which satisfies

$$\triangle u(\mathbf{x}) = 0, \quad \mathbf{x} \in D^+$$

with

$$u(\mathbf{y}) = p(\mathbf{y}), \quad \mathbf{y} \in L.$$

Following Mikhlin (1960), the solution of the interior Dirichlet problem in a multiply-connected domain is sought in the following form:

$$\begin{aligned} u(\mathbf{x}_0) &= \frac{1}{2\pi}\int_L \frac{\partial}{\partial \mathbf{n}(\mathbf{y})}\log|\mathbf{y}-\mathbf{x}_0|\mu(\mathbf{y})\mathrm{d}S(\mathbf{y}) + \sum_{k=1}^{N} a_k \log|\mathbf{x}_0 - \mathbf{s}_k|, \quad \mathbf{x}_0 \in D^+, \\ &= \frac{1}{2\pi}\int_L \frac{1}{r}\frac{\partial r}{\partial \mathbf{n}(\mathbf{y})}\mu(\mathbf{y})\mathrm{d}S(\mathbf{y}) + \sum_{k=1}^{N} a_k \log|\mathbf{x}_0 - \mathbf{s}_k|, \quad r = |\mathbf{y}-\mathbf{x}_0|, \end{aligned} \tag{13}$$

where $\mathbf{s}_k$ is a point inside the curve L_k and $a_k, k = 1, \ldots, N$, are unknown constants. These constants have to be obtained as a part of the solution. The density $\mu(\mathbf{y})$ satisfies the integral equation

$$\mu(\mathbf{y}) = -\frac{1}{\pi}\int_L \frac{1}{r}\frac{\partial r}{\partial \mathbf{n}(\mathbf{y}')}\mu(\mathbf{y}')\mathrm{d}S(\mathbf{y}') + 2h(\mathbf{y}), \tag{14}$$

where

$$h(\mathbf{y}) = p(\mathbf{y}) - \sum_{k=1}^{N} a_k \log|\mathbf{y} - \mathbf{s}_k|.$$

For future reference note that

$$\frac{1}{r}\frac{\partial r}{\partial \mathbf{n}(\mathbf{y}')} = \frac{(y_1' - y_1)n_1(\mathbf{y}') + (y_2' - y_2)n_2(\mathbf{y}')}{|\mathbf{y}' - \mathbf{y}|^2}.$$

It can be observed that there are N independent nontrivial solutions of the homogeneous equation corresponding to Eq. (14) which are given by

$$\begin{aligned} \zeta_i(\mathbf{y}) &= 1, \quad \mathbf{y} \in L_i, \quad i = 1, \ldots, N \\ &= 0, \quad \mathbf{y} \in L_k, \quad i \neq k \quad \text{or} \quad \mathbf{y} \in L_0. \end{aligned} \tag{15}$$

According to the Fredholm alternative, in order for a solution to Eq. (14) to exist, the function $h(\mathbf{y})$ must be orthogonal to $\psi^i(\mathbf{y}), i = 1, \ldots, N$, i.e.

$$\int_L h(\mathbf{y})\psi^i(\mathbf{y})\mathrm{d}S(\mathbf{y}) = 0, \quad i = 1, \ldots, N, \tag{16}$$

where $\psi^i(\mathbf{y})$ are nontrivial solutions of the adjoint equation corresponding to Eq. (14). Note that $\psi^i(\mathbf{y})$ satisfies the equation

$$\psi^i(\mathbf{y}) = -\frac{1}{\pi}\int_L \frac{1}{r}\frac{\partial r}{\partial \mathbf{n}(\mathbf{y})}\psi^i(\mathbf{y}')\mathrm{d}S(\mathbf{y}'), \quad i = 1, \ldots, N.$$

The conditions given by Eq. (16) give rise to N equations which are then used to determine the constants a_k, $k = 1, \ldots, N$.

Again for future reference note that

$$\frac{1}{r}\frac{\partial r}{\partial \mathbf{n}(\mathbf{y})} = \frac{(y_1 - y_1')n_1(\mathbf{y}) + (y_2 - y_2')n_2(\mathbf{y})}{|\mathbf{y}' - \mathbf{y}|^2}.$$

The procedure to calculate the eigenfunctions, $\psi^i(\mathbf{y})$ is adopted from Günter (1967) and is described in detail in Kulkarni (2003). The main points of the procedure are described next.

Consider the following integral equation

$$\phi(\mathbf{y}) = -\lambda \frac{1}{\pi} \int_L \frac{1}{r} \frac{\partial r}{\partial \mathbf{n}(\mathbf{y})} \phi(\mathbf{y}') \mathrm{d}S(\mathbf{y}') + t_i(\mathbf{y}) \tag{17}$$

with $\lambda = 1$. Here $t_i(\mathbf{y})$ is a function defined on the boundary and is given by

$$t_i(\mathbf{y}) = \delta_{ik} \quad \text{if } \mathbf{y} \in L_k. \tag{18}$$

Eq. (17) is solved by assuming that $\phi(\mathbf{y})$ can be written in the following form:

$$\phi(\mathbf{y}) = \rho_0(y) + \lambda \rho_1(\mathbf{y}) + \lambda^2 \rho_2(\mathbf{y}) + \cdots. \tag{19}$$

Substituting Eq. (19) in Eq. (17) and equating equal powers of λ one gets

$$\begin{aligned}
&\rho_0(\mathbf{y}) = t_i(\mathbf{y}),\\
&\rho_1(\mathbf{y}) = -\frac{1}{\pi} \int_L \frac{1}{r} \frac{\partial r}{\partial \mathbf{n}(\mathbf{y})} \rho_0(\mathbf{y}') \mathrm{d}S(\mathbf{y}'),\\
&\rho_2(\mathbf{y}) = -\frac{1}{\pi} \int_L \frac{1}{r} \frac{\partial r}{\partial \mathbf{n}(\mathbf{y})} \rho_1(\mathbf{y}') \mathrm{d}S(\mathbf{y}'),\\
&\vdots\\
&\rho_{2n+1}(\mathbf{y}) = -\frac{1}{\pi} \int_L \frac{1}{r} \frac{\partial r}{\partial \mathbf{n}(\mathbf{y})} \rho_{2n}(\mathbf{y}') \mathrm{d}S(\mathbf{y}'), \qquad (20)\\
&\rho_{2n+2}(\mathbf{y}) = -\frac{1}{\pi} \int_L \frac{1}{r} \frac{\partial r}{\partial \mathbf{n}(\mathbf{y})} \rho_{2n+1}(\mathbf{y}') \mathrm{d}S(\mathbf{y}'). \qquad (21)
\end{aligned}$$

One can then show that for $\lambda = 1$ one has

$$\lim_{n\to\infty} \rho_{2n}(\mathbf{y}) = A_1(\mathbf{y}), \tag{22}$$

$$\lim_{n\to\infty} \rho_{2n+1}(\mathbf{y}) = A_2(\mathbf{y}). \tag{23}$$

and this convergence is uniform. From Eqs. (20), (21) and Eqs. (22), (23) one gets

$$A_2(\mathbf{y}) = -\frac{1}{\pi} \int_L \frac{1}{r} \frac{\partial r}{\partial \mathbf{n}(\mathbf{y})} A_1(\mathbf{y}') \mathrm{d}S(\mathbf{y}'), \tag{24}$$

$$A_1(\mathbf{y}) = -\frac{1}{\pi} \int_L \frac{1}{r} \frac{\partial r}{\partial \mathbf{n}(\mathbf{y})} A_2(\mathbf{y}') \mathrm{d}S(\mathbf{y}'). \tag{25}$$

Adding Eqs. (24) and (25) one gets

$$\psi^i(\mathbf{y}) = -\frac{1}{\pi} \int_L \frac{1}{r} \frac{\partial r}{\partial \mathbf{n}(\mathbf{y})} \psi^i(\mathbf{y}') \mathrm{d}S(\mathbf{y}'),$$

where

$$\psi^i(\mathbf{y}) = A_1(\mathbf{y}) + A_2(\mathbf{y}). \tag{26}$$

Hence $\psi^i(\mathbf{y})$ is the ith eigenfunction of the homogeneous adjoint equation corresponding to Eq. (14) and it has been constructed by choosing $t_i(\mathbf{y})$ defined in Eq. (18).

It can be shown that the N eigenfunctions which are constructed using the above procedure are independent. These eigenfunctions are then used to determine the constants a_k, $k = 1, \ldots, N$ (see Eq. (16)). Once the constants are determined, the BWM can now be applied to obtain $u(\mathbf{x}_0)$ with

$$R(\mathbf{x}_0,\mathbf{y})=\frac{1}{2\pi}\frac{1}{r}\frac{\partial r}{\partial \mathbf{n}(\mathbf{y})},\quad K(\mathbf{y},\mathbf{y}')=-\frac{1}{\pi}\frac{1}{r}\frac{\partial r}{\partial \mathbf{n}(\mathbf{y}')},\quad f(\mathbf{y})=2h(\mathbf{y})\quad\text{and}\quad\lambda=1.$$

Note that the imposition of the constraints leads to the cancellation of the pole at $\lambda=1$ (see Kulkarni, 2003). The solution may still have a pole at $\lambda=-1$ (see Günter, 1967). The solution is therefore modified using pole elimination which consists of multiplying Eq. (3) by $(1+\lambda)$ to cancel the pole. It is then multiplied by $R(\mathbf{x}_0,\mathbf{y}_0)$ and integrated term wise. $u(\mathbf{x}_0)$ is obtained by evaluating the series at $\lambda=1$ and is given by

$$u(\mathbf{x}_0)=\frac{1}{2}I_0(\mathbf{x}_0)+\frac{1}{2}\sum_{n=1}^{\infty}(I_{n-1}(\mathbf{x}_0)+I_n(\mathbf{x}_0)). \tag{27}$$

The individual terms in Eq. (27) are evaluated using the direct estimator given in Section 2.2 and the densities given in Section 2.3.

The method to calculate the constants a_k, $k=1,\ldots,N$, using the BWM is now presented. For simplicity, a doubly-connected domain (i. e. $N=1$) is considered. For this case only one constant, namely a_1, needs to be calculated. From Eq. (16) it is seen that the constant a_1 is given by

$$a_1=\frac{\int_L p(\mathbf{y})\psi^1(\mathbf{y})\mathrm{d}S(\mathbf{y})}{\int_L \log|\mathbf{y}-\mathbf{s}_1|\psi^1(\mathbf{y})\mathrm{d}S(\mathbf{y})}. \tag{28}$$

The eigenfunction $\psi^1(\mathbf{y})$ is generated by defining the function $t_1(\mathbf{y})$ as follows

$$\begin{aligned} t_1(\mathbf{y})&=1,\quad \mathbf{y}\in L_1\\ &=0,\quad \mathbf{y}\in L_0. \end{aligned} \tag{29}$$

Now from Eqs. (22), (23) and (26) one gets

$$\begin{aligned}\int_L p(\mathbf{y})\psi^1(\mathbf{y})\mathrm{d}S(\mathbf{y})&=\int_L p(\mathbf{y})(A_1(\mathbf{y})+A_2(\mathbf{y}))\mathrm{d}S(\mathbf{y})\\ &=\int_L p(\mathbf{y})\Big(\lim_{n\to\infty}\rho_{2n}(\mathbf{y})\Big)\mathrm{d}S(\mathbf{y})+\int_L p(\mathbf{y})\Big(\lim_{n\to\infty}\rho_{2n+1}(\mathbf{y})\Big)\mathrm{d}S(\mathbf{y})\\ &=\lim_{n\to\infty}\underbrace{\int_L p(\mathbf{y})\rho_{2n}(\mathbf{y})\mathrm{d}S(\mathbf{y})}_{\text{Integral 1}}+\lim_{n\to\infty}\underbrace{\int_L p(\mathbf{y})\rho_{2n+1}(\mathbf{y})\mathrm{d}S(\mathbf{y})}_{\text{Integral 2}}. \end{aligned} \tag{30}$$

Similarly,

$$\int_L \log|\mathbf{y}-\mathbf{s}_1|\psi^1(\mathbf{y})\mathrm{d}S(\mathbf{y})=\lim_{n\to\infty}\underbrace{\int_L \log|\mathbf{y}-\mathbf{s}_1|\rho_{2n}(\mathbf{y})\mathrm{d}S(\mathbf{y})}_{\text{Integral3}}+\lim_{n\to\infty}\underbrace{\int_L \log|\mathbf{y}-\mathbf{s}_1|\rho_{2n+1}(\mathbf{y})\mathrm{d}S(\mathbf{y})}_{\text{Integral 4}}. \tag{31}$$

Integral 1 and *Integral 2* defined above are calculated by the BWM with

$$R(\mathbf{x}_0,\mathbf{y})=p(\mathbf{y}),\quad K(\mathbf{y},\mathbf{y}')=-\frac{1}{\pi}\frac{1}{r}\frac{\partial r}{\partial \mathbf{n}(\mathbf{y})},\quad f(\mathbf{y})=t(\mathbf{y})\quad\text{and}\quad\lambda=1.$$

The even terms in the BWM simulation approximate *Integral 1* while the odd terms approximate *Integral 2*. Similarly, *Integral 3* and *Integral 4* defined above are calculated by the BWM with

$$R(\mathbf{x}_0,\mathbf{y})=\log|\mathbf{y}-\mathbf{s}_1|,\quad K(\mathbf{y},\mathbf{y}')=-\frac{1}{\pi}\frac{1}{r}\frac{\partial r}{\partial \mathbf{n}(\mathbf{y})},\quad f(\mathbf{y})=t(\mathbf{y})\quad\text{and}\quad\lambda=1.$$

The even terms in the BWM simulation approximate *Integral 3* while the odd terms approximate *Integral 4*. Note that $R(\mathbf{x}_0, \mathbf{y})$ is the only term which is different in the two sets of parameters given above. Hence the two simulations of the BWM can be carried out simultaneously with an appropriate modification to account for different $R(\mathbf{x}_0, \mathbf{y})$.

The adjoint estimator described in Section 2.2 and the initial and transition densities described in Section 2.3 are used in the Monte Carlo integration.

3.2. Interior Neumann problem in a multiply-connected domain

The interior Neumann problem involves the determination of a function $u(\mathbf{x})$ which satisfies

$$\triangle u(\mathbf{x}) = 0, \quad \mathbf{x} \in D^+,$$

with

$$\frac{\partial u}{\partial \mathbf{n}}(\mathbf{y}) = q(\mathbf{y}), \quad \mathbf{y} \in L \quad \text{and} \quad \int_L q(\mathbf{y}) \mathrm{d}S(\mathbf{y}) = 0.$$

The solution of the interior Neumann problem in a multiply-connected domain (see Fig. 3) is sought in the following form (for e.g., see Mikhlin, 1960):

$$u(\mathbf{x}_0) = \frac{1}{2\pi} \int_L \log|\mathbf{y} - \mathbf{x}_0| \mu(\mathbf{y}) \mathrm{d}S(\mathbf{y}) + \sum_{k=1}^{N} a_k \log|\mathbf{x}_0 - \mathbf{s}_k|, \quad \mathbf{x}_0 \in D^+, \tag{32}$$

where $\mathbf{s}_k$ is a point inside the curve L_k and a_k, $k = 1, \ldots, N$, are constants which are given by

$$a_k = -\frac{1}{2\pi} \int_{L_k} q(\mathbf{y}) \mathrm{d}S(\mathbf{y}), \quad k = 1, \ldots, N. \tag{33}$$

The density $\mu(\mathbf{y})$ satisfies the integral equation

$$\mu(\mathbf{y}) = \frac{1}{\pi} \int_L \frac{1}{r} \frac{\partial r}{\partial \mathbf{n}(\mathbf{y})} \mu(\mathbf{y}') \mathrm{d}S(\mathbf{y}') - 2p(\mathbf{y}), \tag{34}$$

where

$$p(\mathbf{y}) = q(\mathbf{y}) - \sum_{k=1}^{N} a_k \frac{\partial}{\partial \mathbf{n}(\mathbf{y})} \log|\mathbf{y} - \mathbf{s}_k|.$$

The Boundary Walk Method is applied to obtain $u(\mathbf{x}_0)$ with

$$R(\mathbf{x}_0, \mathbf{y}) = \frac{1}{2\pi} \log|\mathbf{y} - \mathbf{x}_0|, \quad K(\mathbf{y}, \mathbf{y}') = -\frac{1}{\pi} \frac{1}{r} \frac{\partial r}{\partial \mathbf{n}(\mathbf{y})}, \quad f(\mathbf{y}) = 2p(\mathbf{y}) \quad \text{and} \quad \lambda = -1.$$

The series given by Eq. (3) does not need any modification for the interior Neunmann problem and can be directly evaluated at $\lambda = -1$ (see Kulkarni, 2003). $u(\mathbf{x}_0)$ is therefore given by

$$u(\mathbf{x}_0) = \sum_{n=0}^{\infty} I_n(\mathbf{x}_0)(-1)^n. \tag{35}$$

The individual terms in Eq. (35) are evaluated using the adjoint estimator given in Section 2.2 and the densities given in Section 2.3.

Remark. Note that the 'log' terms in Eqs. (13) and (32) have an altogether different purpose. It is essential to add them for the Dirichlet problem so as to complete the 'range' of the double layer potential. This is similar to the 'completed double layer method' presented in Power and Miranda (1987), Kim and Karrilla (1991) and others. For the Neumann problem it is not essential to add the 'log' terms. It is still possible to find the solution to the problem using the Boundary Walk Method but then one would have to use the method of pole elimination to remove the pole at $\lambda = 1$. For the solution procedure outlined above, with the choice of a_k's given in Eq. (33), the 'log' terms help to remove the pole at $\lambda = 1$ and hence allows one to directly evaluate the series at $\lambda = -1$.

4. Solutions of problems in linear elasticity using the BWM

This section presents integral formulations for interior displacement and traction prescribed problems which are appropriate for use with the Boundary Walk Method. The procedure to use these formulations in conjunction with the BWM is also described. The formulations are based on weakly singular kernels. The formulation for displacement prescribed problems is given in Kulkarni (2003) and the kernel used in the integral formulation is based on the double layer potential of the second kind as described in Kupradze (1965). The weakly singular formulation for traction prescribed problems is given in Mikhailov (1989).

Note that the direct boundary integral formulation given by Rizzo (1967)

$$\begin{aligned} u_i(\mathbf{x}_0) &= \int_\Gamma \mathbf{U}_{ij}(\mathbf{x}_0,\mathbf{y}) t_j(\mathbf{y}) \mathrm{d}S(\mathbf{y}) - \int_\Gamma \mathbf{T}_{ij}(\mathbf{x}_0,\mathbf{y}) u_j(\mathbf{y}) \mathrm{d}S(\mathbf{y}), \quad \mathbf{x}_0 \in D^+, \\ \frac{u_i(\mathbf{y})}{2} &= \int_\Gamma \mathbf{U}_{ij}(\mathbf{y},\mathbf{y}') t_j(\mathbf{y}') \mathrm{d}S(\mathbf{y}') - \int_\Gamma \mathbf{T}_{ij}(\mathbf{y},\mathbf{y}') u_j(\mathbf{y}') \mathrm{d}S(\mathbf{y}'), \quad \mathbf{y},\mathbf{y}' \in \Gamma \end{aligned} \tag{36}$$

is not appropriate for the application of the BWM. Here $\mathbf{U}(\mathbf{x},\mathbf{y})$ and $\mathbf{T}(\mathbf{x},\mathbf{y})$ are the usual displacement and traction kernels found in the Boundary Element Method (BEM) literature. First observe that the above formulation coupled with BWM can handle only traction prescribed problems since the BWM is a technique to solve integral equations which are of second kind. Further, if one attempts to solve traction prescribed problems by using Eq. (36) in conjunction the BWM, one would have to evaluate the term $\int_\Gamma \mathbf{U}_{ij}(\mathbf{y},\mathbf{y}') t_j(\mathbf{y}') \mathrm{d}S(\mathbf{y}')$ for each different value of $\mathbf{y}$. The number of different $\mathbf{y}$'s would depend on the sample size of the Monte Carlo integration in the BWM. One would either have to use a separate Monte Carlo integration routine each time or would have to evaluate it each time using the procedure followed in the usual BEM. The first choice would lead to a large increase in the computational effort while the second choice would not only lead to an increase in computational effort but would also nullify the advantage of the BWM of avoiding meshing altogether. Another important point to note is that the above formulation is strongly singular ($\mathrm{O}(1/r)$). The difficulty in using a strongly singular formulation with the densities defined earlier is that the estimators (see Eqs. (8) and (11)) have infinite variance. Sabelfeld (1991) has defined new estimators to overcome this problem but it is a computationally expensive task. Another possible way is to use different densities while preserving the earlier definition of the estimators. But then one loses the advantage of working with densities that are very easy to sample from. To overcome the problems associated with using a strongly singular formulation, a weakly singular formulation is used for displacement prescribed and traction prescribed problems. Note that the kernel occurring in the displacement prescribed problems has the form

$$\mathbf{T}_{\mathrm{II}_{ij}}(\mathbf{x},\mathbf{y}) = -\frac{1}{\pi(3-4\nu)} \frac{1}{r} \frac{\partial r}{\partial \mathbf{n}_\mathbf{y}} \left[(1-2\nu)\delta_{ij} + \frac{\partial r}{\partial y_i} \frac{\partial r}{\partial y_j} \right], \quad \mathbf{y} \in \Gamma, \tag{37}$$

while the weakly singular kernel occurring in the traction prescribed problems has the form

$$\mathbf{K}^*_{ij}(\mathbf{x},\mathbf{y}) = -\frac{1}{\pi}\frac{1}{r}\frac{\partial r}{\partial \mathbf{n}_\mathbf{x}}\frac{\partial r}{\partial y_i}\frac{\partial r}{\partial y_j}, \quad \mathbf{x} \in \Gamma.$$

Here $r = |\mathbf{y} - \mathbf{x}|$, $\mathbf{n}(\cdot)$ denotes the outward normal, and μ and ν are the shear modulus and Poisson's ratio, respectively.

4.1. Displacement prescribed problem in a multiply-connected domain

Consider a homogeneous isotropic elastic solid with Lamé constants λ and μ occupying the region D^+ shown in Fig. 3. Under a small deformation field, the interior displacement problem in the absence of body forces involves the determination of a function $\mathbf{u}(\mathbf{x})$ which satisfies

$$\mu\Delta\mathbf{u}(\mathbf{x}) + (\lambda+\mu)\nabla(\nabla\cdot\mathbf{u}(\mathbf{x})) = \mathbf{0}, \quad \mathbf{x} \in D^+ \tag{38}$$

with

$$\lim_{\substack{\mathbf{x}\in D^+ \\ \mathbf{x}\to\mathbf{y}\in L}} \mathbf{u}(\mathbf{x}) = \mathbf{g}(\mathbf{y}).$$

The displacement is represented in the following form (see Kulkarni, 2003)

$$\mathbf{u}(\mathbf{x}_0) = -\int_L \mathbf{T}_{\mathrm{II}}(\mathbf{x}_0,\mathbf{y})\boldsymbol{\mu}(\mathbf{y})\mathrm{d}S(\mathbf{y}) + \sum_{k=1}^{N}\mathbf{U}(\mathbf{x}_0,\mathbf{s}_k)\mathbf{a}_\mathbf{k}, \quad \mathbf{x}_0 \in D^+, \tag{39}$$

where $\mathbf{s}_k$ is a point inside the curve L_k (see Fig. 3) and $\mathbf{a}_k$, $k = 1,\ldots,N$, are constant vectors which are to be determined during the solution procedure.

The density $\boldsymbol{\mu}$ satisfies the integral equation

$$\boldsymbol{\mu}(\mathbf{y}) = \int_L 2\mathbf{T}_{\mathrm{II}}(\mathbf{y},\mathbf{y}')\boldsymbol{\mu}(\mathbf{y}')\mathrm{d}S(\mathbf{y}') + 2\mathbf{f}(\mathbf{y}), \tag{40}$$

where

$$\mathbf{f}(\mathbf{y}) = \mathbf{g}(\mathbf{y}) - \sum_{k=1}^{N}\mathbf{U}(\mathbf{y},\mathbf{s}_k)\mathbf{a}_k.$$

It is shown in Kulkarni (2003) that there are $2N$ nontrivial solutions of the homogeneous equation corresponding to Eq. (40) and they are of the form

$$\boldsymbol{\zeta}_i(\mathbf{y}) = [\,\delta_{((i+1)/2)k} \quad \delta_{((i/2)k)}\,]^{\mathrm{T}}, \quad \mathbf{y} \in L_k, \quad k = 0,1,\ldots,N.$$

Note that where n is not an integer, δ_{nk} is defined to be 0. Therefore, according to the Fredholm alternative, in order for a solution to Eq. (40) to exist, the function $\mathbf{f}(\mathbf{y})$ must be orthogonal to $\boldsymbol{\varphi}_i(\mathbf{y}), i = 1,\ldots,2N$, i.e.

$$\int_L \boldsymbol{\varphi}_i^{\mathrm{T}}(\mathbf{y})\mathbf{f}(\mathbf{y})\mathrm{d}S(\mathbf{y}) = 0, \tag{41}$$

where $\boldsymbol{\varphi}_i(\mathbf{y})$ is the nonzero solution of

$$\boldsymbol{\varphi}_i(\mathbf{y}) = \int_L 2\mathbf{T}^*_{\mathrm{II}}(\mathbf{y},\mathbf{y}')\boldsymbol{\varphi}_i(\mathbf{y}')\mathrm{d}S(\mathbf{y}'). \tag{42}$$

Here $\mathbf{T}^*_{\mathrm{II}}(\mathbf{y},\mathbf{y}')$ is the adjoint kernel corresponding to $\mathbf{T}_{\mathrm{II}}(\mathbf{y},\mathbf{y}')$. The conditions given by Eq. (41) give rise to $2N$ equations which are then used to determine the constant vectors, $\mathbf{a}_k$, $k = 1,\ldots,N$. This situation is similar to the one encountered when solving the interior Dirichlet problem in multiply-connected domains. As before, one first constructs the eigenfunctions $\boldsymbol{\varphi}_i(\mathbf{y})$, $i = 1,\ldots,2N$. Since the form of the eigenfunctions

of the weakly singular kernel is similar to those of the kernel used in the Dirichlet problem, a method similar to the one described in Section 3.1 is used to calculate the eigenfunctions of the adjoint kernel $\mathbf{T}^{*}_{\mathrm{II}}(\mathbf{y},\mathbf{y}')$.

Consider the following integral equation

$$\boldsymbol{\phi}(\mathbf{y}) = \lambda \int_L 2\mathbf{T}^{*}_{\mathrm{II}}(\mathbf{y},\mathbf{y}')\boldsymbol{\phi}(\mathbf{y}')\mathrm{d}S(\mathbf{y}') + \mathbf{t}_i(\mathbf{y}) \tag{43}$$

with $\lambda = 1$. Here

$$\mathbf{t}_i(\mathbf{y}) = [\,\delta_{((i+1)/2)k} \quad \delta_{((i/2)k)}\,]^{\mathrm{T}}, \quad k = 0, 1, \ldots, N. \tag{44}$$

Note that where n is not an integer, δ_{nk} is defined to be 0. The solution to Eq. (43) is sought in form of a series shown below

$$\boldsymbol{\phi}(\mathbf{y}) = \boldsymbol{\rho}_0(\mathbf{y}) + \lambda\boldsymbol{\rho}_1(\mathbf{y}) + \lambda^2\boldsymbol{\rho}_2(\mathbf{y}) + \cdots \tag{45}$$

One can then show that

$$\lim_{n\to\infty} \boldsymbol{\rho}_{2n}(\mathbf{y}) = \mathbf{A}_{i1}(\mathbf{y}), \tag{46}$$

$$\lim_{n\to\infty} \boldsymbol{\rho}_{2n+1}(\mathbf{y}) = \mathbf{A}_{i2}(\mathbf{y}). \tag{47}$$

and that the convergence is uniform. Note that the i in the subscript denotes the fact that these functions are generated using the function $\mathbf{t}_i(\mathbf{y})$. One then observes that the function $\boldsymbol{\varphi}_i(\mathbf{y})$ given by

$$\boldsymbol{\varphi}_i(\mathbf{y}) = \mathbf{A}_{i1}(\mathbf{y}) + \mathbf{A}_{i2}(\mathbf{y}) \tag{48}$$

is the ith eigenfunction of the homogeneous equation corresponding to Eq. (43) which has been constructed by choosing the function $\mathbf{t}_i(\mathbf{y})$ defined by Eq. (44). The eigenfunctions $\boldsymbol{\varphi}_i(\mathbf{y}), i = 1, \ldots, 2N$, are used in conjunction with the conditions given by Eq. (41) to determine the constants $\mathbf{a}_k, k = 1, \ldots, N$. Once the constants are determined, the BWM can now be applied to obtain $\mathbf{u}(\mathbf{x}_0)$ with

$$\mathbf{R}(\mathbf{x}_0,\mathbf{y}) = -\mathbf{T}_{\mathrm{II}}(\mathbf{x}_0,\mathbf{y}), \quad \mathbf{K}(\mathbf{y},\mathbf{y}') = 2\mathbf{T}_{\mathrm{II}}(\mathbf{y},\mathbf{y}'), \quad \mathbf{f}(\mathbf{y}) = 2\mathbf{g}(\mathbf{y}) \quad \text{and} \quad \lambda = 1.$$

Note that the fulfilling of the conditions given by Eq. (41) leads to the cancellation of the pole at $\lambda = 1$. This situation is similar to the one encountered in the Dirichlet problem. The pole at $\lambda = -1$ is eliminated by the pole elimination technique. Finally, $\mathbf{u}(\mathbf{x}_0)$ is given by

$$\mathbf{u}(\mathbf{x}_0) = \frac{1}{2}\mathbf{I}_0(\mathbf{x}_0) + \frac{1}{2}\sum_{n=1}^{\infty}(\mathbf{I}_{n-1}(\mathbf{x}_0) + \mathbf{I}_n(\mathbf{x}_0)). \tag{49}$$

The individual terms in Eq. (49) are then estimated using the direct estimator defined in Section 2.2 and the densities defined in Section 2.3.

The method to calculate the constants $\mathbf{a}_k$, $k = 1, \ldots, N$, using the Boundary Walk Method, is now outlined. For simplicity a doubly-connected domain is considered. For this problem a constant $\mathbf{a}_1$ vector which has two components, say a_{11} and a_{21}, needs to be determined. One has to solve a system of equations which can be written as

$$\begin{bmatrix} C_{11} & C_{12} \\ C_{21} & C_{22} \end{bmatrix} \begin{bmatrix} a_{11} \\ a_{21} \end{bmatrix} = \begin{bmatrix} d_1 \\ d_2 \end{bmatrix}, \tag{50}$$

where

$$C_{ij} = \int_L \boldsymbol{\varphi}_i^{\mathrm{T}}(\mathbf{y})\mathbf{U}_{(:,j)}(\mathbf{y},\mathbf{s}_1)\mathrm{d}S(\mathbf{y}) = \int_L \mathbf{U}_{(j,:)}(\mathbf{y},\mathbf{s}_1)\boldsymbol{\varphi}_i(\mathbf{y})\mathrm{d}S(\mathbf{y})$$

and

$$d_i = \int_L \boldsymbol{\varphi}_i^{\mathrm{T}}(\mathbf{y})\mathbf{g}(\mathbf{y})\mathrm{d}S(\mathbf{y}) = \int_L \mathbf{g}^{\mathrm{T}}(\mathbf{y})\boldsymbol{\varphi}_i(\mathbf{y})\mathrm{d}S(\mathbf{y}).$$

Observe that

$$[\, C_{i1} \quad C_{i2}\,]^{\mathrm{T}} = \int_L \mathbf{U}(\mathbf{y},\mathbf{s}_1)\boldsymbol{\varphi}_i(\mathbf{y})\mathrm{d}S(\mathbf{y}).$$

The eigenfunctions $\boldsymbol{\varphi}_i(\mathbf{y})$, $i = 1, 2$, are generated by using the function $\mathbf{t}_i(\mathbf{y})$ defined in Eq. (44). From Eqs. (47)–(51), one gets

$$\begin{aligned}
[\, C_{i1} \quad C_{i2}\,]^{\mathrm{T}} &= \int_L \mathbf{U}(\mathbf{y},\mathbf{s}_1)\boldsymbol{\varphi}_i(\mathbf{y})\mathrm{d}S(\mathbf{y}) = \int_L \mathbf{U}(\mathbf{y},\mathbf{s}_1)(\mathbf{A}_{i1}(\mathbf{y}) + \mathbf{A}_{i2}(\mathbf{y}))\mathrm{d}S(\mathbf{y}) \\
&= \int_L \mathbf{U}(\mathbf{y},\mathbf{s}_1)\Big(\lim_{n\to\infty}\boldsymbol{\rho}_{2n}(\mathbf{y})\Big)\mathrm{d}S(\mathbf{y}) + \int_L \mathbf{U}(\mathbf{y},\mathbf{s}_1)\Big(\lim_{n\to\infty}\boldsymbol{\rho}_{2n+1}(\mathbf{y})\Big)\mathrm{d}S(\mathbf{y}) \\
&= \lim_{n\to\infty}\underbrace{\int_L \mathbf{U}(\mathbf{y},\mathbf{s}_1)\boldsymbol{\rho}_{2n}(\mathbf{y})\mathrm{d}S(\mathbf{y})}_{\text{Integral } i1} + \lim_{n\to\infty}\underbrace{\int_L \mathbf{U}(\mathbf{y},\mathbf{s}_1)\boldsymbol{\rho}_{2n+1}(\mathbf{y})\mathrm{d}S(\mathbf{y})}_{\text{Integral } i2}.
\end{aligned} \tag{51}$$

Similarly one has

$$d_i = \int_L \mathbf{g}^{\mathrm{T}}(\mathbf{y})\boldsymbol{\varphi}_i(\mathbf{y})\mathrm{d}S(\mathbf{y}) = \lim_{n\to\infty}\underbrace{\int_L \mathbf{g}^{\mathrm{T}}(\mathbf{y})\boldsymbol{\rho}_{2n}(\mathbf{y})\mathrm{d}S(\mathbf{y})}_{\text{Integral}i3} + \lim_{n\to\infty}\underbrace{\int_L \mathbf{g}^{\mathrm{T}}(\mathbf{y})\boldsymbol{\rho}_{2n+1}(\mathbf{y})\mathrm{d}S(\mathbf{y})}_{\text{Integral}i4}. \tag{52}$$

Integral i1 and *Integral i2* defined above are calculated by the BWM with

$$R(\mathbf{x}_0,\mathbf{y}) = \mathbf{U}(\mathbf{y},\mathbf{s}_1), \quad K(\mathbf{y},\mathbf{y}') = 2\mathbf{T}^*_{\mathrm{II}}(\mathbf{y},\mathbf{y}'), \quad f(\mathbf{y}) = \mathbf{t}_i(\mathbf{y}) \quad \text{and} \quad \lambda = 1.$$

The even terms in the BWM simulation approximate *Integral i1* while the odd terms approximate *Integral i2*. Similarly, *Integral i3* and *Integral i4* defined above are calculated by the BWM with

$$R(\mathbf{x}_0,\mathbf{y}) = \mathbf{g}^{\mathrm{T}}(\mathbf{y}), \quad K(\mathbf{y},\mathbf{y}') = 2\mathbf{T}^*_{\mathrm{II}}(\mathbf{y},\mathbf{y}'), \quad f(\mathbf{y}) = \mathbf{t}_i(\mathbf{y}) \quad \text{and} \quad \lambda = 1.$$

The even terms in the BWM simulation approximate *Integral i3* while the odd terms approximate *Integral i4*. Note that two simulations of the BWM are needed to be carried out as there are two eigenfunctions which must be generated.

4.2. Traction prescribed problem in a multiply-connected domain

Again consider a homogeneous isotropic elastic solid with Lamé constants λ and μ occupying the region D^+ shown in Fig. 3. Under a small deformation field, the interior traction problem in the absence of body forces involves the determination of a function $\mathbf{u}(\mathbf{x})$ which is unique up to an additive constant (or the corresponding unique stress field) which satisfies

$$\mu\Delta\mathbf{u}(\mathbf{x}) + (\lambda+\mu)\nabla(\nabla\cdot\mathbf{u}(\mathbf{x})) = \mathbf{0}, \quad \mathbf{x}\in D^+ \tag{53}$$

with

$$\lim_{\substack{\mathbf{x}\in D^+\\ \mathbf{x}\to\mathbf{y}\in L}} \mathbf{T}^n(\mathbf{u}(\mathbf{x})) = \mathbf{t}(\mathbf{y})$$

where $\mathbf{T}^n(\cdot)$ is the traction operator. The weakly singular kernel used for the displacement problem is not suitable for the traction prescribed problem. This is because the concept of pseudo-traction, which is used in deriving the kernel, has no physical interpretation (see for e.g. Kupradze, 1965). Therefore, the weakly singular formulation presented in Mikhailov (1989) is used as the starting point for the application of the Boundary Walk Method to solve traction prescribed problems in multiply-connected two-dimensional domains. Following Mikhailov (1989), the stress at a point $\mathbf{x}_0$ is written as

$$\sigma_{il}(\mathbf{x}_0) = \int_L \mathbf{S}_{ilj}(\mathbf{x}_0,\mathbf{y}) f_j(\mathbf{y}) \mathrm{d}S(\mathbf{y}) + 2\mu \sum_{k=1}^{N} b_k \left[\frac{\partial (V_k)_i}{\partial x_0 l} + \frac{\partial (V_k)_l}{\partial x_0 i} \right] + 2\mu \sum_{k=1}^{N} \left(a_{1k} \left[\frac{\partial (U_k^1)_i}{\partial x_0 l} + \frac{\partial (U_k^1)_l}{\partial x_0 i} \right] + a_{2k} \left[\frac{\partial (U_k^2)_i}{\partial x_0 l} + \frac{\partial (U_k^2)_l}{\partial x_0 i} \right] \right) + \lambda \delta_{il} \sum_{k=1}^{N} \left(a_{1k} \left[\frac{\partial (U_k^1)_1}{\partial x_0 1} + \frac{\partial (U_k^1)_2}{\partial x_0 2} \right] + a_{2k} \left[\frac{\partial (U_k^2)_1}{\partial x_0 1} + \frac{\partial (U_k^2)_2}{\partial x_0 2} \right] \right), \tag{54}$$

where

$$\mathbf{S}_{ilj}(\mathbf{x}_0,\mathbf{y}) = \frac{1}{\pi} \frac{1}{r} \frac{\partial r}{\partial y_i} \frac{\partial r}{\partial y_l} \frac{\partial r}{\partial y_j}, \quad r = |\mathbf{y} - \mathbf{x}_0|,$$

$$\mathbf{V}_k(\mathbf{x}_0) = \begin{bmatrix} \dfrac{x_{01} - s_{k1}}{2\mu r_k^2} & \dfrac{x_{02} - s_{k2}}{2\mu r_k^2} \end{bmatrix}^{\mathrm{T}}, \quad r_k = |\mathbf{x}_0 - \mathbf{s}_k|,$$

$$\mathbf{U}_k^1 = \mathbf{U}(\mathbf{s}_k, \mathbf{x}_0)(:,1), \quad \mathbf{U}_k^2 = \mathbf{U}(\mathbf{s}_k, \mathbf{x}_0)(:,2)$$

and

$$a_{ik} = \int_{L_k} t_i(\mathbf{y}) \mathrm{d}S(\mathbf{y}).$$

Here $\mathbf{U}(\mathbf{s}_k, \mathbf{x}_0)$ is the usual displacement kernel, $\mathbf{s}_k$ is a point inside the curve L_k, t_i is the ith component of the prescribed traction and b_k, $k = 1, \ldots, N$, are unknown constants which are to be determined during the solution procedure. The density $f_i(\mathbf{y})$ satisfies the equation

$$f_i(\mathbf{y}) = -\int_L 2\mathbf{K}_{ij}^*(\mathbf{y},\mathbf{y}') f_j(\mathbf{y}') \mathrm{d}S(\mathbf{y}') + 2g_i(\mathbf{y}). \tag{55}$$

Here

$$\mathbf{K}_{ij}^*(\mathbf{y},\mathbf{y}') = -\frac{1}{\pi} \frac{1}{r} \frac{\partial r}{\partial \mathbf{n}(\mathbf{y})} \frac{\partial r}{\partial y_i} \frac{\partial r}{\partial y_j}, \quad r = |\mathbf{y}' - \mathbf{y}|,$$

$$g_i(\mathbf{y}) = t_i(\mathbf{y}) - 2\mu \sum_{k=1}^{N} b_k \left[\frac{\partial (V_k)_i}{\partial y_l} + \frac{\partial (V_k)_l}{\partial y_i} \right] n_l(\mathbf{y}) - 2\mu \sum_{k=1}^{N} \left(a_{1k} \left[\frac{\partial (U_k^1)_i}{\partial y_l} + \frac{\partial (U_k^1)_l}{\partial y_i} \right] + a_{2k} \left[\frac{\partial (U_k^2)_i}{\partial y_l} + \frac{\partial (U_k^2)_l}{\partial y_i} \right] \right) n_l(\mathbf{y}) + \lambda \delta_{il} \sum_{k=1}^{N} \left(a_{1k} \left[\frac{\partial (U_k^1)_1}{\partial y_1} + \frac{\partial (U_k^1)_2}{\partial y_2} \right] + a_{2k} \left[\frac{\partial (U_k^2)_1}{\partial y_1} + \frac{\partial (U_k^2)_2}{\partial y_2} \right] \right) n_l(\mathbf{y}).$$

Note that $\mathbf{K}^*(\mathbf{y},\mathbf{y}')$ is a weakly singular kernel. It can be verified (see Kim and Karrilla, 1991) that there are $N + 3$ eigenfunctions of the homogeneous equation corresponding to Eq. (55) and N of the eigenfunctions, $\boldsymbol{\psi}_i(\mathbf{y})$, $i = 1, \ldots, N$, are given by

$$\psi_i(\mathbf{y}) = \mathbf{n}(\mathbf{y}), \quad \mathbf{y} \in L_i$$
$$= \mathbf{0} \qquad \text{otherwise.}$$

Therefore, according to the Fredholm alternative, in order for a solution to Eq. (55) to exist, the function $\mathbf{g}(\mathbf{y})$ must be orthogonal to $\boldsymbol{\varphi}_i(\mathbf{y})$, $i = 1, \ldots, N+3$, i.e.

$$\int_L \boldsymbol{\varphi}_i^{\mathrm{T}}(\mathbf{y})\mathbf{g}(\mathbf{y})\mathrm{d}S(\mathbf{y}) = 0, \tag{56}$$

where $\boldsymbol{\varphi}_i(\mathbf{y})$ is the nonzero solution of

$$\boldsymbol{\varphi}_i(\mathbf{y}) = -\int_L 2\mathbf{K}(\mathbf{y}, \mathbf{y}')\boldsymbol{\varphi}_i(\mathbf{y}')\mathrm{d}S(\mathbf{y}'). \tag{57}$$

Here $\mathbf{K}(\mathbf{y}, \mathbf{y}')$ is the adjoint kernel corresponding to the kernel $\mathbf{K}^*(\mathbf{y}, \mathbf{y}')$. Noting that three of the $N+3$ nonzero solutions of Eq. (57) are given by

$$[1 \quad 0]^{\mathrm{T}}, \quad [0 \quad 1]^{\mathrm{T}} \quad \text{and} \quad [y_2 \quad -y_1]^{\mathrm{T}}$$

it is seen that three of the conditions on the function $\mathbf{g}(\mathbf{y})$ given by Eq. (56) are equivalent to

$$\int_L g_1(\mathbf{y})\mathrm{d}S(\mathbf{y}) = 0, \quad \int_L g_2(\mathbf{y})\mathrm{d}S(\mathbf{y}) = 0, \quad \text{and} \quad \int_L (y_2\, g_1(\mathbf{y}) - y_1\, g_2(\mathbf{y}))\mathrm{d}S(\mathbf{y}) = 0.$$

It is observed that the function $\mathbf{g}(\mathbf{y})$ identically satisfies the above conditions and hence these 3 conditions are not useful in determining the constants b_k, $k = 1, \ldots, N$. The remaining N conditions give rise to N equations which are then used to determine the constants b_k, $k = 1, \ldots, N$. The procedure to calculate the remaining N eigenfunctions of Eq. (57) is outlined below and it based on the method described in Section 3.1.

Consider the following integral equation:

$$\boldsymbol{\phi}(\mathbf{y}) = \lambda \int_L 2\mathbf{K}(\mathbf{y}, \mathbf{y}')\boldsymbol{\phi}(\mathbf{y}')\mathrm{d}S(\mathbf{y}') + \mathbf{h}_i(\mathbf{y}) \tag{58}$$

with $\lambda = -1$. Here the functions $\mathbf{h}_i(\mathbf{y})$, $i = 1, \ldots, N$ are defined as follows:

$$\begin{aligned} \mathbf{h}_i(\mathbf{y}) &= \mathbf{n}(\mathbf{y}), \quad \mathbf{y} \in L_i \\ &= \mathbf{0} \qquad \text{otherwise.} \end{aligned} \tag{59}$$

The solution to Eq. (58) is sought in form of a series shown below

$$\boldsymbol{\phi}(\mathbf{y}) = \boldsymbol{\rho}_0(\mathbf{y}) + \lambda\boldsymbol{\rho}_1(\mathbf{y}) + \lambda^2\boldsymbol{\rho}_2(\mathbf{y}) + \cdots. \tag{60}$$

Proceeding in the manner presented in Section 3.1, one can show that

$$\lim_{n\to\infty} \boldsymbol{\rho}_{2n}(\mathbf{y}) = \mathbf{B}_{i1}(\mathbf{y}), \tag{61}$$

$$\lim_{n\to\infty} \boldsymbol{\rho}_{2n+1}(\mathbf{y}) = \mathbf{B}_{i2}(\mathbf{y}) \tag{62}$$

and that the convergence is uniform. Note that the i in the subscript denotes the fact that these functions are generated using the function $\mathbf{h}_i(\mathbf{y})$. One then observes that the function $\boldsymbol{\varphi}_i(\mathbf{y})$ given by

$$\boldsymbol{\varphi}_i(\mathbf{y}) = \mathbf{B}_{i1}(\mathbf{y}) - \mathbf{B}_{i2}(\mathbf{y}) \tag{63}$$

is the ith eigenfunction of the equation given by Eq. (57) which has been constructed by choosing the function $\mathbf{h}_i(\mathbf{y})$ defined by Eq. (59). The eigenfunctions $\boldsymbol{\varphi}_i(\mathbf{y})$, $i = 1, \ldots, N$, are used in conjunction with the

conditions given by Eq. (56) to determine the constants b_k, $k = 1, \ldots, N$. Once the constants are determined, the BWM is now applied with

$$\mathbf{R}(\mathbf{x}_0, \mathbf{y}) = \mathbf{S}(\mathbf{x}_0, \mathbf{y}), \quad \mathbf{K}(\mathbf{y}, \mathbf{y}') = 2\mathbf{K}^*(\mathbf{y}, \mathbf{y}'), \quad \mathbf{f}(\mathbf{y}) = 2\mathbf{t}(\mathbf{y}) \quad \text{and} \quad \lambda = -1.$$

Note that the components of stress are represented in a form of a vector $\boldsymbol{\sigma}$. Also note that the fulfilling of the conditions given by Eq. (56) lead to the cancellation of the pole at $\lambda = -1$. This situation is similar to the one encountered in the Neumann problem. The pole at $\lambda = 1$ is eliminated by the pole elimination technique and $\boldsymbol{\sigma}(\mathbf{x}_0)$ is then given by

$$\boldsymbol{\sigma}(\mathbf{x}_0) = \frac{1}{2}\mathbf{I}_0(\mathbf{x}_0) + \frac{1}{2}\sum_{n=1}^{\infty}(\mathbf{I}_n(\mathbf{x}_0) - \mathbf{I}_{n-1}(\mathbf{x}_0))(-1)^n. \tag{64}$$

The individual terms in Eq. (64) are then estimated using the adjoint estimator defined in Section 2.2 and densities defined in Section 2.3.

The constants b_k, $k = 1, \ldots, N$, can be determined using the BWM in a manner similar to the one outlined in Section 3.1 taking into account the matrix structure of the kernels and the function $\mathbf{h}(\mathbf{y})$ defined in Eq. (59).

5. Numerical results

The Boundary Walk Method is used to solve some simple illustrative problems in potential theory and the calculated results are compared with the exact solution in each case.

Remark. There are two important issues to consider when computing the result using a series expansion in which individual terms are calculated using Monte Carlo integration.

(a) The number of the terms in a series, n.
(b) The number of samples N, to evaluate the individual terms in the series.

The coefficient of variation (CV) is used to decide the number of terms k to be considered for the solution. First, a fixed number of terms of the series, say n, are calculated using a fixed N. Here a large N is used so that the CV for the first few terms is relatively small. The CV is then calculated for all the n terms. The first k terms are chosen if the |CV| for the $(k+1)$th term is greater than 1.0.

Note. It is observed that for all problems defined in multiply-connected domains, the standard deviation $\widehat{s}_t$, increases with successive terms and a proof explaining this observation is given in Appendix A.

5.1. Potential theory-interior Dirichlet problem

The BWM is used to solve the Dirichlet problem in an annular region bounded by two concentric circles with $r_1 = 0.5$ and $r_0 = 2.0$ with boundary conditions $u(0.5, \theta) = 0.0$ and $u(2.0, \theta) = 100.0$ respectively. The exact solution is as follows

$$u(r, \theta) = 50.0\left(\frac{\log(r)}{\log(r_0)} + 1\right).$$

Before solving the Dirichlet problem, the constant a_1 is evaluated using the procedure described in Section 3.1. The point $\mathbf{s}_1$ is assumed to be located at the origin. Table 1 gives the approximations for the successive terms in the numerator and the denominator.

Table 1
Calculation of a_1

Term	Numerator			Denominator		
	Mean	$\widehat{s_t}$	CV	Mean	$\widehat{s_t}$	CV
0	0.00000	0.00000	–	−2.17240	0.00332	−0.00153
1	−627.35162	1.18374	−0.00189	−6.51721	0.00996	−0.00153
2	2.28755	2.50425	1.09473	−2.15514	0.02085	−0.00967
3	−628.19138	4.99613	−0.00795	−6.53585	0.04157	−0.00636

Monte Carlo simulation parameters : $N = 8,000,000$, $n = 4$, CV = 1.

It is observed from Table 1 that the standard deviation of the successive terms increases. It is also seen that the mean of the alternate terms remains approximately constant for the terms where the CV is low. Since the CV is lowest in magnitude for the first two terms, the constant a_1, for this particular example, is approximated as (see Eq. (28) and Eqs. (30) and (31)

$$a_1 = \frac{(0.00000) + (-627.35162)}{(-2.17240) + (-6.51721)} = 72.19560.$$

As mentioned Section 3.1, the even numbered terms (including the zeroth term) in the column *Numerator* approximate *Integral 1* while the odd numbered terms approximate *Integral 2*. Similarly the even numbered terms (including the zeroth term) in the column *Denominator* approximate *Integral 3* while the odd numbered terms approximate *Integral 4*. Note that for this particular example, the exact value of a_1 is 72.1369. Using the value a_1 calculated using the BWM, the results of the Dirichlet problem at the points

$$x = r(r_0 \cos(\theta)),$$

$$y = r(r_0 \sin(\theta))$$

are presented in Table 2.

It is seen from Table 2 that the computed results are quite accurate and also have a low CV.

5.2. Potential theory-interior Neumann problem

The BWM is used to solve the Neumann problem in the domain shown in Fig. 4. The following exact solution is assumed:

$$u(r, \theta) = r\cos(\theta) + \log(r).$$

The normal derivative corresponding to the above solution is prescribed on the boundary. Since the solution is unique up to an additive constant, the gradient of $u(r, \theta)$ in the x-direction is calculated here. The results at points

$$x = r(r_0 \cos(\theta)),$$

Table 2
Solution $u(x, y)$ of the Dirichlet problem at $\theta = \pi/4$

r	k	Computed value	S.D.	CV	Exact value	% Error
0.3	1	13.06027	0.03210	0.00246	13.15172	0.695
0.6	1	63.11582	0.01972	0.00031	63.15172	0.057
0.9	2	92.45437	0.07430	0.00080	92.39984	0.059

Monte Carlo simulation parameters: $N = 4,000,000$, $n = 5$, CV = 1.

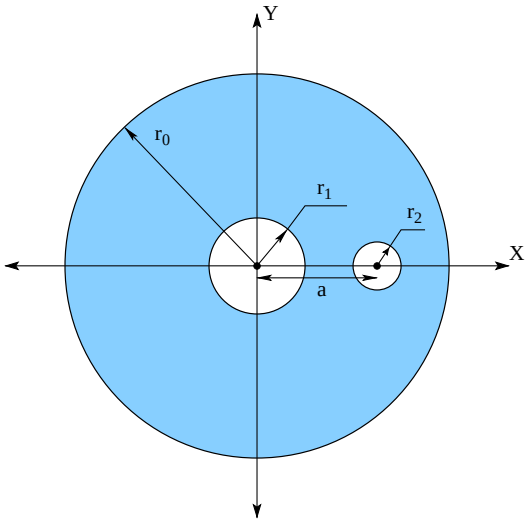

Fig. 4. Domain for the Neumann problem $r_0 = 2.0$, $r_1 = 0.5$, $r_2 = 0.25$, $a = 1.0$.

$$y = r(r_0 \sin(\theta))$$

are presented in Table 3.

For the present problem, the point $\mathbf{s}_1$ is assumed to be located at the origin while the point $\mathbf{s}_2$ is assumed to be located at the center of the circle with radius r_2. The two constants, a_1 and a_2, are calculated using Eq. (33) and are $a_1 = -1.0$ and $a_2 = 0.0$.

It is again observed from Table 3 that the computed results are quite accurate with a low CV.

5.3. Linear elasticity-displacement prescribed problem

The BWM is used to solve a plane strain displacement prescribed problem in an annular ring bounded by two concentric circles with $r_1 = 0.5$ and $r_0 = 2.0$. The shear modulus, μ, and Poisson's ratio, v, of the annular ring are 1.0 and 0.3, respectively. The following boundary conditions are imposed:

On the outer boundary

$$u(2.0, \theta) = (3 - 4v)\log(2.0) - \cos^2(\theta) + \cos(\theta),$$

$$v(2.0, \theta) = -\sin(\theta)\cos(\theta) + \sin(\theta).$$

On the inner boundary

$$u(0.5, \theta) = (3 - 4v)\log(0.5) - \cos^2(\theta),$$

Table 3
Solution $\frac{\partial u(x,y)}{\partial x}$ of the Neumann problem at $\theta = \pi/4$

r	k	Computed value	S.D.	CV	Exact value	% Error
0.3	3	2.18829	0.01992	0.00910	2.17851	0.449
0.6	4	1.56908	0.03744	0.02386	1.58926	1.270
0.9	4	1.44591	0.03398	0.02350	1.39284	3.810

Monte Carlo simulation parameters: $N = 4,000,000$, $n = 5$, CV = 1.

$$v(0.5,\theta) = -\sin(\theta)\cos(\theta).$$

The exact solution is as follows:

$$u(r,\theta) = (3-4v)\log(r) - \cos^2(\theta) + w(r)\cos(\theta),$$

$$v(r,\theta) = -\sin(\theta)\cos(\theta) + w(r)\sin(\theta),$$

where

$$w(r) = \frac{1}{(r_0^2 - r_1^2)}\left(2r - \frac{0.5}{r}\right).$$

Before solving the problem, the constant vector $\mathbf{a}_1$ is evaluated using the procedure described in Section 4.1. The point $\mathbf{s}_1$ is assumed to be located at the origin. The Monte Carlo simulation parameters used in the calculation of the constants in Eq. (50) are as follows: $N = 4,000,000$, $n = 6$ and CV = 1. The simulation is run twice as explained in Section 4.1. The constants are calculated using the second and third term in the simulation (for the numbering convention, please refer to Table 1). The constants are given by

$$C_{11} = 0.69946, \quad C_{12} = 0.0, \quad d_1 = -12.14292,$$

$$C_{21} = 0.0, \quad C_{22} = 0.73033, \quad d_2 = 0.0$$

The constant vector is therefore given by

$$\mathbf{a}_1 = [\,-17.36042 \quad 0.0\,]^{\mathrm{T}}.$$

This value compares reasonably well with the value $[-17.59292\ 0.0]^{\mathrm{T}}$ which is given by a different method proposed in Kulkarni (2003). This method is again based on the weakly singular kernel and is similar to the one proposed by Mikhlin (1960) for solving interior Dirichlet problems in multiply-connected domains. Using the value of $\mathbf{a}_1$ calculated using the BWM, the results for the displacement problem at the points

$$x = r(r_0\cos(\theta)),$$

$$y = r(r_0\sin(\theta))$$

are presented in Table 4.

As is seen from the Table 4, the results compare favourably with the exact results. One important point to note is the high CV and errors for those displacement components which have a 'small' magnitude. In most engineering applications, the quantity with the largest magnitude is generally of interest and therefore it is felt the inability of the BWM to capture 'small' quantities well should not be considered as a severe shortcoming of the method.

Table 4
Solution of a displacement problem at $\theta = \pi/4$

r		k	Computed value	S.D.	CV	Exact value	% Error
0.3	u	2	−1.32730	0.00327	0.00246	−1.35035	1.707
	v	2	−0.42781	0.00359	0.00839	−0.43086	0.708
0.6	u	5	0.18746	0.04352	0.23216	0.20216	7.271
	v	5	−0.12651	0.05621	0.44431	−0.12602	0.397
0.9	u	6	1.20524	0.05449	0.04521	1.18446	1.754
	v	6	0.13680	0.05434	0.39722	0.12644	8.194

Monte Carlo simulation parameters: $N = 4,000,000$, $n = 6$, CV = 1.0.

5.4. Linear elasticity-traction prescribed problem

The BWM is used to find stresses at different points in a square plate with a central circular hole which is submitted to uniform unit traction in the x-direction (see Fig. 5). Note that the dimension of the plate is large when compared with radius of the hole. The shear modulus, μ, and Poisson's ratio, ν, of the plate are 1.0 and 0.3, respectively. The computed values of the stress components are compared with the analytical solution obtained for a circular hole in an infinite plate subjected to farfield traction. This comparison is valid for the current problems for points which are 'close' to the hole. The stresses at points close to the hole and along the y-axis are then given by (see for e.g. Timoshenko and Goodier, 1970)

$$\boldsymbol{\sigma}_{xx}(0,y) = \frac{1}{2}\left(2 + \frac{a^2}{y^2} + 3\frac{a^4}{y^4}\right),$$

$$\boldsymbol{\sigma}_{yy}(0,y) = \frac{3}{2}\left(\frac{a^2}{y^2} - \frac{a^4}{y^4}\right),$$

$$\boldsymbol{\sigma}_{xy}(0,y) = 0.$$

Before solving the problem, the constants a_{11}, a_{21} and b_1 need to be evaluated (see Eq. (54)). Since the hole is traction free, $a_{11} = 0$ and $a_{21} = 0$. The constant b_1 is evaluated using a procedure similar to the one described in Section 3.1. The point $\mathbf{s}_1$ is assumed to be located at the origin. The Monte Carlo simulation parameters used in the calculation of the constant b_1 are as follows: $N = 4,000,000$, $n = 4$ and CV $= 1$. The constant is calculated using the zeroth and first term in the simulation (for the numbering convention, please refer to Table 1). The constant b_1 is given by $b_1 = 0.50069$. Using this value of the constant, stresses at different points along the y-axis are calculated using the BWM and results are presented in Table 5. Note that only the $\boldsymbol{\sigma}_{xx}$ and $\boldsymbol{\sigma}_{yy}$ stresses are reported.

It is observed from Table 5 that the stress of primary practical importance, viz. $\boldsymbol{\sigma}_{xx}$, is estimated reasonably accurately with the BWM while a significant error is observed in one of the results for the smaller stress component $\boldsymbol{\sigma}_{yy}$. Again, it is felt that since this is of little practical importance, it should not be considered a severe shortcoming of the BWM.

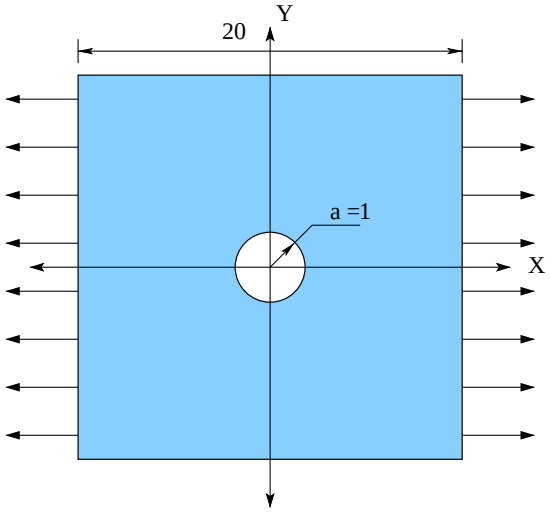

Fig. 5. Square plate with a central hole.

Table 5
Solution of the traction problem

y		k	Computed value	S.D.	CV	Exact value	% Error
1.5	σ_{xx}	5	1.54690	0.05353	0.03460	1.51851	1.870
	σ_{yy}	4	0.45772	0.05399	0.11795	0.37037	23.585
2.0	σ_{xx}	5	1.24227	0.02414	0.01943	1.21875	1.930
	σ_{yy}	4	0.28325	0.03735	0.13186	0.28125	0.711
2.5	σ_{xx}	4	1.15880	0.00798	0.00689	1.11840	3.612
	σ_{yy}	3	0.20553	0.00963	0.04685	0.20160	1.949

Monte Carlo simulation parameters: $N = 4,000,000$, $n = 6$, CV = 1.0.

6. Concluding remarks

The primary aim of the present paper is to present the theoretical details of a local method called the Boundary Walk Method (BWM) and to give appropriate integral formulations for both potential theory and linear elasticity which can be used with the BWM. Simple illustrative problems with available closed form solutions are also solved using the BWM to show the feasibility the method for solving problem in multiply-connected domains. To the best of the authors' knowledge, this paper presents, for the first time, numerical results for problems in linear elasticity in multiply-connected domains using a local method with an appropriate integral formulation. The numerical results are in reasonable agreement with the exact solutions. To further develop the method and to efficiently exploit some of its advantages (e.g. locality, no meshing) the issues mentioned below need to be carefully addressed.

1. It is proved that the estimators when used with the current densities lead to random variables with the property

$$\lim_{k\to\infty} \mathrm{Var}[\zeta_k] = \infty.$$

   This leads to to a large sample size even to estimate the first few terms with a small variance. To overcome this problem, the issue of selecting a proper estimator and/or different densities needs to be investigated.
2. Integral formulations that can solve mixed boundary value problems with the the BWM need to be developed.
3. The robustness of the method needs to be investigated along with the sensitivity of the solution to different constants which have to be found during the course of application of the BWM.

Acknowledgements

This research has been supported by NSF Grant CMS-9912524 to Cornell University. The computing for this research was carried out using the resources of the Cornell Theory Center, which receives funding from Cornell University, New York State, the National Center for Research Resources at the National Institutes of Health, the National Science Foundation, the Defense Department Modernization program, the United States Department of Agriculture, and corporate partners.

Appendix A

It was mentioned in Section 5 that the standard deviation of the sample mean of the individual terms increases with successive terms when solving problems in nonconvex or multiply-connected regions. The following proof attempts to explain the phenomenon of increasing standard deviation. The proof is given for the case of the interior Dirichlet problem in a multiply-connected region and the main conclusion drawn is that the densities used (see Section 2.3) are the cause of increasing variance. Similar proofs can also be given for the observed increasing variance when solving other problems in nonconvex and multiply-connected domains using either the direct estimator or the adjoint estimator along with the densities given in Section 2.3.

As mentioned in Section 3.1, the direct estimator given by Eq. (8) is used in the case of interior Dirichlet problem to estimate the individual terms. The random variable given by Eq. (7) is used to define the direct estimator. The random variable defined by Eq. (7) is rewritten below for a quick reference.

$$\zeta_k = \frac{R(\mathbf{x}_0, \mathbf{Y}_0)}{p_0(\mathbf{Y}_0)} W_k f(\mathbf{Y}_k), \tag{A.1}$$

with

$$W_k = W_{k-1} \frac{K(\mathbf{Y}_{k-1}, \mathbf{Y}_k)}{p(\mathbf{Y}_k | \mathbf{Y}_{k-1})}, \quad W_0 \equiv 1. \tag{A.2}$$

The constraints on the densities (see Section 2.2) ensure that the random variable given above has a finite mean and in fact the definition of the random variable implies that

$$E[\zeta_k] = I_k(\mathbf{x}_0) \tag{A.3}$$

with

$$I_k(\mathbf{x}_0) = \underbrace{\int_\Gamma \cdots \int_\Gamma}_{k+1 \text{ times}} R(\mathbf{x}_0, \mathbf{y}_0) K(\mathbf{y}_0, \mathbf{y}_1) \cdots K(\mathbf{y}_{k-1}, \mathbf{y}_k) f(\mathbf{y}_k) \mathrm{d}S(\mathbf{y}_k) \cdots \mathrm{d}S(\mathbf{y}_1) \mathrm{d}S(\mathbf{y}_0).$$

The proof of Eq. (A.3) is as follows. Using Eqs. (A.2), (A.1) can be written as

$$\zeta_k = \frac{R(\mathbf{x}_0, \mathbf{Y}_0)}{p_0(\mathbf{Y}_0)} \frac{K(\mathbf{Y}_0, \mathbf{Y}_1)}{p(\mathbf{Y}_1 | \mathbf{Y}_0)} \cdots \frac{K(\mathbf{Y}_{k-1}, \mathbf{Y}_k)}{p(\mathbf{Y}_k | \mathbf{Y}_{k-1})} f(\mathbf{Y}_k). \tag{A.4}$$

Therefore

$$\begin{aligned} E[\zeta_k] = & \underbrace{\int_\Gamma \cdots \int_\Gamma}_{k+1 \text{ times}} \frac{R(\mathbf{x}_0, \mathbf{y}_0)}{p_0(\mathbf{y}_0)} \frac{K(\mathbf{y}_0, \mathbf{y}_1)}{p(\mathbf{y}_1 | \mathbf{y}_0)} \cdots \frac{K(\mathbf{y}_{k-2}, \mathbf{y}_{k-1})}{p(\mathbf{y}_{k-1} | \mathbf{y}_{k-2})} \\ & \times \frac{K(\mathbf{y}_{k-1}, \mathbf{y}_k)}{p(\mathbf{y}_k | \mathbf{y}_{k-1})} f(\mathbf{y}_k) p_0(\mathbf{y}_0) p(\mathbf{y}_1 | \mathbf{y}_0) \cdots p(\mathbf{y}_k | \mathbf{y}_{k-1}) \mathrm{d}S(\mathbf{y}_k) \cdots \mathrm{d}S(\mathbf{y}_1) \mathrm{d}S(\mathbf{y}_0) \\ = & \underbrace{\int_\Gamma \cdots \int_\Gamma}_{k+1 \quad \text{times}} R(\mathbf{x}_0, \mathbf{y}_0) K(\mathbf{y}_0, \mathbf{y}_1) \cdots K(\mathbf{y}_{k-1}, \mathbf{y}_k) f(\mathbf{y}_k) \mathrm{d}S(\mathbf{y}_k) \cdots \mathrm{d}S(\mathbf{y}_1) \mathrm{d}S(\mathbf{y}_0) = I_k(\mathbf{x}_0), \end{aligned} \tag{A.5}$$

which proves Eq. (A.3).

The variance of the random variable ζ_k is given by

$$\mathrm{Var}[\zeta_k] = E[\zeta_k^2] - E[\zeta_k]^2. \tag{A.6}$$

The second term in Eq. (A.6) is the square of the integral $I_k(\mathbf{x}_0)$ and is bounded. Using Eq. (A.4), the first term in Eq. (A.6) can be written as

$$E[\zeta_k^2] = \underbrace{\int_\Gamma \cdots \int_\Gamma}_{k+1\text{times}} \frac{R^2(\mathbf{x}_0,\mathbf{y}_0)}{p_0^2(\mathbf{y}_0)} \frac{K^2(\mathbf{y}_0,\mathbf{y}_1)}{p^2(\mathbf{y}_1\,|\,\mathbf{y}_0)} \cdots \frac{K^2(\mathbf{y}_{k-2},\mathbf{y}_{k-1})}{p^2(\mathbf{y}_{k-1}\,|\,\mathbf{y}_{k-2})}$$
$$\times \frac{K^2(\mathbf{y}_{k-1},\mathbf{y}_k)}{p^2(\mathbf{y}_k\,|\,\mathbf{y}_{k-1})} f^2(\mathbf{y}_k) p_0(\mathbf{y}_0) p(\mathbf{y}_1\,|\,\mathbf{y}_0) \cdots p(\mathbf{y}_k\,|\,\mathbf{y}_{k-1}) \mathrm{d}S(\mathbf{y}_k) \cdots \mathrm{d}S(\mathbf{y}_1) \mathrm{d}S(\mathbf{y}_0).$$

From the expression of the density given in Section 2.3, one gets

$$\frac{R^2(\mathbf{x}_0,\mathbf{y}_0)}{p_0^2(\mathbf{y}_0)} = \frac{(|\cos(\phi_{\mathbf{y}_0,\mathbf{x}_0})|/(2\pi r))^2}{(\cos(\phi_{\mathbf{y}_0,\mathbf{x}_0})/(\Omega_{\mathbf{x}_0} r))^2} = \frac{\Omega_{\mathbf{x}_0}^2}{(2\pi)^2} = c_{\mathbf{x}_0},$$

$$\frac{K^2(\mathbf{y}_{k-1},\mathbf{y}_k)}{p^2(\mathbf{y}_k\,|\,\mathbf{y}_{k-1})} = \frac{(|\cos(\phi_{\mathbf{y}_k,\mathbf{y}_{k-1}})|/(\pi r))^2}{(\cos(\phi_{\mathbf{y}_{k-1},\mathbf{y}_k})/(\Omega_{\mathbf{y}_{k-1}} r))^2} = \frac{\Omega_{\mathbf{y}_{k-1}}^2}{\pi^2} = c_{\mathbf{y}_{k-1}}.$$

From the definition of the total solid angle it follows that for interior problems $c_{\mathbf{x}_0} \geqslant 1$ and $c_{\mathbf{y}_{k-1}} \geqslant 1$ where the equality holds for only a simply-connected convex domain. Also $c_{\mathbf{y}_{k-1}} \geqslant c_{\mathbf{ymin}} \geqslant 1$ where

$$c_{\mathbf{ymin}} = \frac{\Omega_{\mathbf{ymin}}^2}{\pi^2}.$$

Here **ymin** is a point on the boundary where the total angle subtended by the boundary is the minimum. Let $c_{\min} = \min(c_{\mathbf{x}_0}, c_{\mathbf{ymin}})$. Similarly $1 \leqslant c_{\mathbf{y}_{k-1}} \leqslant c_{\mathbf{ymax}}$ where

$$c_{\mathbf{ymax}} = \frac{\Omega_{\mathbf{ymax}}^2}{\pi^2}.$$

Here **ymax** is a point on the boundary where the total angle subtended by the boundary is the maximum. Let $c_{\max} = \max(c_{\mathbf{x}_0}, c_{\mathbf{ymax}})$. Therefore it follows that for nonconvex or multiply-connected domains

$$c_{\min}^{(k+1)} I_{k+1}[f](\mathbf{x}_0) < E[\zeta_k^2] < c_{\max}^{(k+1)} I_{k+1}[f](\mathbf{x}_0), \tag{A.7}$$

where

$$I_{k+1}[f](\mathbf{x}_0) = \underbrace{\int_\Gamma \cdots \int_\Gamma}_{k+1\text{ times}} f^2(\mathbf{y}_k) p_0(\mathbf{y}_0) p(\mathbf{y}_1\,|\,\mathbf{y}_0) \cdots p(\mathbf{y}_k\,|\,\mathbf{y}_{k-1}) \mathrm{d}S(\mathbf{y}_k) \cdots \mathrm{d}S(\mathbf{y}_1) \mathrm{d}S(\mathbf{y}_0).$$

Note that for such domains, $c_{\min} > 1$ and $c_{\max} > 1$. It is observed from the definition of $I_{k+1}[f]$ that

$$I_{k+1}[f](\mathbf{x}_0) = I_k[f](\mathbf{x}_0) = \cdots = I_0[f](\mathbf{x}_0) = E[f^2\,|\,\mathbf{x}_0]. \tag{A.8}$$

Therefore it follows from Eqs. (A-7), (A-8) that the term $E[\zeta_k^2]$ increases with k for nonconvex or multiply-connected domains. For the case of the interior Dirichlet problem, the series given by Eq. (3) is modified by multiplying by $(\lambda + 1)$ to eliminate the pole at $\lambda = -1$. Therefore the modified series (see Section 3.1) is uniformly convergent at $\lambda = 1$. Since the terms in the modified series (see Eq. (27)) tend to zero, the absolute value of the terms in the original series (see Eq. (3)) approaches a constant i.e. $|I_k(\mathbf{x}_0)| = |E[\zeta_k]|$ approaches a constant. Therefore the variance which is given by Eq. (A-6) increases monotonically with k for nonconvex or multiply-connected domains i.e.

$$\mathrm{Var}[\zeta_{k+1}] > \mathrm{Var}[\zeta_k] \quad k = 0, 1, \ldots$$

and

$$\lim_{k\to\infty} \mathrm{Var}[\zeta_k] = \infty.$$

It is seen from the proof that the main reason the variance increases for nonconvex or multiply-connected domains is because of the fact that $c_{\min} > 1$. The reason $c_{\min}$ is always greater than 1 is due fact that the densities are based on distributing the boundary point uniformly in the solid angle subtended by the boundary at a point.

Remark. Note that other densities, namely those which lead to a uniform distribution over the boundary were also tried, but the results obtained were worse than those presented because of the fact that the densities did not cancel the weak singularity present in the kernel. The appropriate choice of a density that would control the variance remains an open question.

References

Evans, M., Swartz, T., 2000. Approximating Integrals via Monte Carlo and Deterministic Methods. Oxford University Press, Oxford.

Günter, N.M., 1967. Potential Theory. Frederick Ungar Publishing Co., New York.

Kim, S., Karrilla, S.J., 1991. Microhydrodynamics: Principles and Selected Applications. Butterworth-Heinemann, Boston.

Kulkarni, S.S., 2003. Integral equation methods to solve problems in two-dimensional potential theory and linear elasticity. PhD. Dissertation, Cornell University.

Kulkarni, S.S., Mukherjee, S., Grigoriu, M., 2003. Local solutions in potential theory and linear elasticity using Monte Carlo Methods. ASME Journal of Applied Mechanics 70, 408–417.

Kupradze, V.D., 1965. Potential methods in the theory of elasticity. Israel Program for Scientific Translations, Jerusalem.

Mikhailov, S.E., 1989. Spectral properties and solution methods for some integral equations of elasticity for plane non-simply-connected bodies with corner points under forces specified on the boundary. Mechanics of Solids 24, 53–63.

Mikhlin, S.G., 1960. Linear Integral Equations. Hindustan Publishing Corporation, Delhi.

Power, H., Miranda, G., 1987. Second kind integral equation formulation of Stoke's flow past a particle of arbitrary shape. SIAM Journal of Applied Mathematics 47, 689–698.

Rizzo, F.J., 1967. An integral equation approach to boundary value problems of classical elastostatics. Quarterly Journal of Applied Mathematics 25, 83–95.

Rubinstein, R.Y., 1981. Simulation and the Monte Carlo Method. John Wiley and Sons, New York.

Sabelfeld, K.K., 1991. Monte Carlo Methods in Boundary Value Problems. Springer-Verlag, Berlin.

Sabelfeld, K.K., Simonov, N.A., 1994. Random Walks on Boundary for Solving PDEs. VSP, Utrecht, Netherlands.

Shia, D., Hui, C., 2000. A Monte Carlo solution method for linear elasticity. International Journal of Solids and Structures 37, 6085–6105.

Sobolev, S.L., 1964. Partial Differential Equations of Mathematical Physics. Dover Publications, New York.

Timoshenko, S.P., Goodier, J.N., 1970. Theory of Elasticity, third ed. McGraw-Hill, New York.